Replication of Boid Inclusion Body Disease-Associated Arenaviruses Is Temperature Sensitive in both Boid and Mammalian Cells

Hepojoki, J ; Kipar, A ; Korzyukov, Y ; Bell-Sakyi, L ; Vapalahti, O ; Hetzel, U

Abstract: UNLABELLED Boid inclusion body disease (BIDB) is a fatal disease of boid snakes, the etiology of which has only recently been revealed following the identification of several novel arenaviruses in diseased snakes. BIBD-associated arenaviruses (BIBDAV) are genetically divergent from the classical Old and New World arenaviruses and also differ substantially from each other. Even though there is convincing evidence that BIBDAV are indeed the etiological agent of BIBD, the BIBDAV reservoir hosts-if any exist besides boid snakes themselves-are not yet known. In this report, we use University of Helsinki virus (UHV; a virus that we isolated from a Boa constrictor with BIBD) to show that BIBDAV can also replicate effectively in mammalian cells, including human cells, provided they are cultured at 30°C. The infection induces the formation of cytoplasmic inclusion bodies (IB), comprised mainly of viral nucleoprotein (NP), similar to those observed in BIBD and in boid cell cultures. Transferring infected cells from 30°C to 37°C ambient temperature resulted in progressive declines in IB formation and in the amounts of viral NP and RNA, suggesting that BIBDAV growth is limited at 37°C. These observations indirectly indicate that IB formation is linked to viral replication. In addition to mammalian and reptilian cells, UHV infected arthropod (tick) cells when grown at 30°C. Even though our findings suggest that BIBDAV have a high potential to cross the species barrier, their inefficient growth at mammalian body temperatures indicates that the reservoir hosts of BIBDAV are likely species with a lower body temperature, such as snakes. IMPORTANCE The newly discovered boid inclusion body disease-associated arenaviruses (BIBDAV) of reptiles have drastically altered the phylogeny of the family Arenavirus. Prior to their discovery, known arenaviruses were considered mainly rodent-borne viruses, with each arenavirus species having its own reservoir host. BIBDAV have so far been demonstrated in captive boid snakes, but their possible reservoir host(s) have not yet been identified. Here we show, using University of Helsinki virus as a model, that these viruses are able to infect mammalian (including human) and arthropod cells. Our results provide in vitro proof of the considerable ability of arenaviruses to cross species barriers. However, our data indicate that BIBDAV growth occurs at 30°C but is inhibited at 37°C, implying that crossing of the species barrier would be hindered by the body temperature of mammalian species.

DOI: https://doi.org/10.1128/JVI.03119-14

Hepojoki, J; Kipar, A; Korzyukov, Y; Bell-Sakyi, L; Vapalahti, O; Hetzel, U (2015). Replication of Boid Inclusion Body Disease-Associated Arenaviruses Is Temperature Sensitive in both Boid and Mammalian Cells. Journal of Virology, 89(2):1119-1128.
DOI: https://doi.org/10.1128/JVI.03119-14

Replication of Boid Inclusion Body Disease Associated Arenaviruses is Temperature Sensitive in Both Boid and Mammalian Cells

Jussi Hepojoki[1#], Anja Kipar[2,3,4], Yegor Korzyukov[1], Lesley Bell-Sakyi[5], Olli Vapalahti[1,4,6] and Udo Hetzel[2,4]

[1]Department of Virology, Infection Biology Research Program, Haartman Institute, University of Helsinki, Helsinki, Finland.

[2]Institute of Veterinary Pathology, Vetsuisse Faculty, University of Zurich, Zurich, Switzerland

[3]Department of Infection Biology, Institute of Global Health, University of Liverpool, Liverpool, UK

[4]Department of Veterinary Biosciences, University of Helsinki, Helsinki, Finland

[5]The Pirbright Institute, Pirbright, UK

[6]Helsinki University Central Hospital Laboratory Division, Helsinki, Finland

Running title: Temperature dependent growth of BIBDAV

[#]*Corresponding author*

Mailing address: **Department of Virology**
Haartman Institute
P.O. Box 21
Haartmaninkatu 3
FI-00014 University of Helsinki
Finland
***Phone:* +358-9-19126**
***Fax:* +358-9-191 26491**
E-mail: jussi.hepojoki@helsinki.fi

Words in text: 5927
Words in abstract: 241
Words in importance: 131

ABSTRACT

Boid inclusion body disease (BIDB) is a fatal disease of boid snakes, the etiology of which has only recently been revealed following identification of several novel arenaviruses in diseased snakes. BIBD-associated arenaviruses (BIBDAV) are genetically divergent from the "classical" Old and New World arenaviruses and also differ substantially from each other. Even though there is convincing evidence that BIBDAV are indeed the etiological agent of BIBD, the BIBDAV reservoir hosts – if any exist besides boid snakes themselves – are not yet known. In this report we use University of Helsinki virus (UHV) to show that BIBDAV can effectively replicate also in mammalian, including human cells provided they are cultured at 30°C. The infection induces the formation of cytoplasmic inclusion bodies (IB), comprised mainly of viral nucleoprotein (NP), similar to those observed in BIBD and in boid cell cultures. Transfer of infected cells from 30°C to 37°C ambient temperature resulted in a progressive decline in IB formation and in the amount of viral NP and RNA, suggesting that BIBDAV growth is limited at 37°C. These observations indirectly indicate that IB formation is linked to viral replication. In addition to mammalian and reptilian cells, UHV infected arthropod (tick) cells when grown at 30°C. Even though our findings suggest that BIBDAV have a high potential to cross the species barrier, their inefficient growth at mammalian body temperatures indicates that the reservoir hosts of BIBDAV are likely species with a lower body temperature such as snakes.

IMPORTANCE

The newly-discovered boid inclusion body disease-associated arenaviruses (BIBDAV) of reptiles have drastically altered the phylogeny of the family *Arenavirus*. Prior to their discovery, known arenaviruses were considered as mainly rodent-borne viruses, with each arenavirus species having its own reservoir host. BIBDAV have so far been demonstrated in captive boid snakes but their possible reservoir host(s) have not yet been identified. Here we show, using University of Helsinki virus as a model, that these viruses are able to infect mammalian (including human) and arthropod cells. Our results provide *in vitro* proof of the considerable ability of arenaviruses to cross species barrier. However, our data indicate BIBDAV growth occurs at 30˚C but is inhibited at 37˚C, implying that crossing of the species barrier would be hindered by the body temperature of mammalian species.

INTRODUCTION

Arenavirus is the genus in the family *Arenaviridae*, RNA viruses that have earlier been described as almost exclusively rodent-borne (1). Several arenaviruses are known to be able to cross the species barrier, for instance to be transmitted from a rodent host to humans (2-4). Such cross-species transmission often leads to severe infections which manifest as hemorrhagic fever (Lassa, Guanarito, Junin, Lujo, Machupo, Sabia or Whitewater Arroyo virus) or meningitis (lymphocytic choriomeningitis virus, LCMV) in humans (1, 5, 6). While these are usually dead-end events for the virus, they can occasionally lead to prolonged transmission chains between humans (7). More recently, several arenaviruses have been detected in snakes with boid inclusion body disease (BIBD) (8-10), and *in vitro* experiments, together with statistical associations, provided convincing evidence of an etiological relationship between BIBD and arenavirus infection (10). The pathomorphology of BIBD is manifested by the development of typical eosinophilic intracytoplasmic inclusion bodies (IB) in almost all cell types of affected animals (10-12). The IB consist predominantly, if not entirely, of a 68-kDa protein (11) that has recently been identified as the arenavirus nucleoprotein (NP) (10). They most likely represent complexes required for arenavirus replication (13).

Arenaviruses have a bi-segmented genome with ambisense coding strategy (14). The L segment encodes the RNA-dependent RNA polymerase (RdRp) and the Z protein, and the S segment encodes the glycoprotein precursor (GPC) and the NP (14). Of these, the RdRp is considered the most conserved, whereas all other structural proteins exhibit a relatively high variability (14, 15). BIBD-associated arenaviruses (BIBDAV) show very high genome variability, particularly in the GPC region (8-10, 16, 17). This may reflect differences between reservoir hosts of the viruses (17), since

59 the glycoproteins encoded in the GPC mediate binding of the virions to the cellular
60 receptor(s) (18).
61 To evaluate the potential of BIBDAV to cross species barriers and to shed some light
62 on the potential reservoir hosts of these viruses, we screened a range of vertebrate and
63 arthropod cell lines for their susceptibility to the University of Helsinki virus (UHV),
64 a virus that we isolated from a *Boa constrictor* with BIBD (10). We also studied the
65 effect of temperature on the growth of BIBDAV, since we earlier observed productive
66 UHV infection in Vero E6 cells only when grown at 27-30˚C (10).
67

MATERIALS AND METHODS

Viruses and cell lines.

UHV propagated in the boid kidney cells (described in (10)), named I/1Ki, used in this study was purified by density gradient ultracentrifugation as described (19) and stored at -70˚C (supplemented with bovine serum albumin, BSA) until used for inoculation. The purified UHV (GenBank accession numbers: KF297881.1 and KF297880.1) was initially used to infect Vero E6 cells (10), and adaptation to Vero E6 cells was enhanced by three consecutive passages (a fresh batch of Vero E6 cells was infected each time with supernatant collected 12-15 days post infection (dpi)). A second BIBDAV isolate, T10404 (from snake no. 5 in (10), GenBank accession number KF564801), was passaged once in the boid kidney cells, concentrated, purified, and stored as described above.

African green monkey kidney (Vero and Vero E6, both from ATCC), human lung adenocarcinoma (A549, from ATCC), baby hamster kidney (BHK-21, from ATCC) and *Boa constrictor* kidney (I/1Ki, described in (10)) cells were cultured in Basal Medium Eagle (BME; Biochrom) containing 10% tryptose phosphate broth (TPB; Difco, Sigma-Aldrich), 15 mM HEPES, 2 mM L-glutamine, 10 µg/ml gentamicin, and 50 IU/ml nystatin (Valeant Pharmaceuticals), pH 7.2 to 7.3 when used for infections with UHV purified from boid cells, and were cultured in Minimal Essential Medium (MEM, Sigma-Aldrich) supplemented with 10% fetal bovine serum (FBS), 25 mM HEPES, 2 mM L-glutamine, 100 IU/ml penicillin, and 100 µg/ml streptomycin when used for infections with UHV purified from Vero E6 cells and infections with T10404. When studying the effect of a temperature switch on BIBDAV growth in vertebrate cells, both infected and non-infected cells were maintained at either 30°C or 37°C for 4 to 5 d after virus inoculation, after which half

of each group of cells at each temperature, infected and non-infected, were transferred to the opposite temperature, i.e. cells grown at 30°C were maintained at 37°C and vice versa. For western blotting and RT-PCR, cell samples were collected at 1-2 d intervals, and samples for other assays (histology and immunohistochemistry) were collected 4 d after the temperature swap. Cells maintained at 30°C or 37°C for the entire experimental period served as controls.

Three tick embryo-derived cell lines, the *Ixodes ricinus* cell line IRE/CTVM19 (20, 21), the *Rhipicephalus* (*Boophilus*) *microplus* cell line BME/CTVM2 (22) and the *Rhipicephalus appendiculatus* cell line RAE/CTVM1 (22) were maintained in 2 ml L-15 (Leibovitz) medium (Sigma-Aldrich) supplemented with 20% FBS, 10% TPB, 2 mM L-glutamine, 100 IU/ml penicillin, and 100 μg/ml streptomycin in sealed flat-sided culture tubes (Nunc) at 30°C. Medium was changed weekly by removal and replacement of ¾ of the medium volume and resuspended cells were subcultured 1:1 when required (20). Infection of tick cells was done by adding UHV propagated in boid cells and purified by density gradient ultracentrifugation to the culture medium, followed by 14 d incubation at 30°C.

Cloning, production and purification of recombinant UHV proteins.

Partial S segment of UHV cloned (10) into pGEM-T vector (Promega) was used as the template for PCR cloning of full length (rNP, amino acids 1-582) as well as N- (rNP-N, amino acids 1-339) and C-terminal (rNP-C, amino acids 346-582) portions of the UHV NP. These regions were chosen based on both the knowledge of functional domains (23) and the structural data of arenavirus NP (24). PCR cloning of the fragments was accomplished using Phusion High-Fidelity DNA polymerase (Thermo Scientific) with the following primers for NP: 5'-GGTACCATGGCTGCACTACAAAGAGC-3' and 5'-

CTCGAGGACCTCCACAGGCC-3'; N-term NP: 5'-GGTACCATGGCTGCACTACAAAGAGC-3' and 5'-CTCGAGCCTTCTCAAACGGAATACCG-3'; C-term NP: 5'-CATATGAGGTTATACCCGGACTTGATGGA-3' and 5'-CTCGAGGACCTCCACAGGCC-3'. The cloning and production of recombinant bacmids was done following the Bac-to-Bac HBM TOPO Secreted expression system manual (Life Technologies). P1 supernatants containing recombinant baculoviruses were harvested 4 to 7 days after transfecting Sf9 cells with purified recombinant bacmids.

For recombinant protein production, confluent High Five cells (75 cm^2 bottle) were detached with a cell scraper and pelleted by centrifugation (500 x g, 5 min, RT). The cell pellets were suspended in 1 ml of cell culture supernatant containing recombinant baculoviruses, incubated for 1 h at room temperature (RT), and transferred into two 175 cm^2 bottles to which 25 ml growth medium were added. The cells were collected between 5 and 7 dpi.

The recombinant proteins were purified from cells infected with recombinant baculovirus as follows: the cell pellet was suspended in 3 ml lysis buffer 1 (50 mM Tris, pH 7.5), and the cell suspension centrifuged (4,000 x g, 10 min, RT). The resultant pellet (containing the insoluble recombinant protein) was suspended in 5 ml lysis buffer 1 and centrifuged as above. The resultant pellet was suspended in 5 ml lysis buffer 2 (50 mM Tris, 150 mM NaCl, 0.1% Triton X-100, pH 7.5) and centrifuged (4,000 x g, 30 min, 4˚C); the procedure was repeated once. After washes with lysis buffer 2 the resultant pellet was suspended in 2 ml lysis buffer 3 (50 mM Tris, 500 mM NaCl, 1% Triton X-100, pH 7.5) and centrifuged (16,000 x g, 5 min, RT). The washing was repeated once using 3 ml lysis buffer 3. The resultant pellet

was homogenized in 9 ml binding buffer (50 mM Tris, 500 mM NaCl, 6 M guanidine-HCl, pH 8.0) by passing several times through an 18G needle on a 5 ml syringe. One ml of Ni-NTA agarose beads (Invitrogen) equilibrated in binding buffer was added to the cell homogenate, followed by 1 h incubation at RT. The beads were washed 3 times with binding buffer (500 x g, 3 min, RT, centrifugations), and the recombinant proteins were eluted by addition of 1 ml elution buffer (50 mM Tris, 500 mM NaCl, 6 M Guanidine-HCl, 500 mM Imidazole, pH 8.0) and centrifugation 500 x g, (3 min, RT). The elution was repeated three times. Concentration and buffer exchange (to 35 mM HEPES, 135 mM NaCl, 1 M guanidine-HCL, pH 8.2) of the recombinant proteins was done using a centrifugal filter device with 10 kDa cut-off (Millipore). For SDS-PAGE analysis, guanidine was removed with ethanol (1 part protein solution + 9 parts ethanol) precipitation (30 min at -70˚C, centrifugation at 16,000 x g for 10 min at 4˚C).

Antibodies.

Purified rNP-N and rNP-C were used to produce polyclonal antisera, similarly to those described in (10), by BioGenes GmbH, but with initial injections of 150 µg, 70 µg boosters on days 7 and 14, 150 µg boosters on day 28, and 70 µg boosters on day 42. A previously prepared rabbit antiserum against purified and lysed UHV (10), and the antisera produced against rNP-N and rNP-C were affinity purified by rNP coupled to CnBr activated Sepharose (GE Healthcare) according to the manufacturer's protocol. The affinity purified rNP-N and rNP-C polyclonal antibodies (PAb) were labeled with horseradish peroxidase (HRP) using the EZ-Link Activated Peroxidase Antibody Labeling Kit (ThermoScientific) as instructed by the manual.

SDS-PAGE and immunoblotting.

Protein separations by SDS-PAGE (8 to 12% gels) and wet blotting of proteins onto nitrocellulose (Whatman) were done according to standard protocols. The protein concentrations of cell lysates (in 50 mM Tris, 150 mM NaCl, 1% Triton X-100, pH 8.0, supplemented with EDTA-free protease inhibitor cocktail, Roche) were determined using the BCA Protein Assay Kit (Pierce, Thermo Scientific), and 10 µg of total protein was loaded for each lane. Sample preparation for SDS-PAGE and immunoblotting as well as the probing and detection of immunoblots using the anti-rNP PAb (affinity purified from anti-UHV serum, used at 0.1 µg/ml concentration) were as described (10). The HRP-labelled anti-rNP-N and anti-rNP-C PAb were used at 0.25 µg/ml to 0.1 µg/ml concentrations diluted in blocking buffer (50 mM Tris, 150 mM NaCl, 0.05% Tween 20, pH 8.0) with 3% skimmed milk powder. The results were recorded on X-ray film (Fuji Medical RX) utilizing in-house ECL reagents.

Quantitative PCR (qPCR).

Total RNA was isolated from UHV-infected boid cells grown at different temperatures with the RNeasy Mini Kit (Qiagen) according to the manufacturer's protocol. For RNA quantification 1 µg total RNA was transcribed to cDNA, using RevertAid Premium Reverse Transcriptase (Thermo Scientific) following the manufacturer's protocol. An equal amount of cDNA from each sample was used as template for real-time PCR (Stratagene MX3500P) amplification of UHV L-segment RNA (primer sequences targeting the Z protein region, originally designed for cloning, Forward: 5'-CATATGAGCGAATCAACCGCAATAGGTC-3' and Reverse: 5'-CTCGAGTGGT TCGGGGAGG-3'), with Maxima SYBR Green qPCR Master Mix (Thermo Scientific). The relative amount of viral RNA was estimated based on Ct differences as compared to the lowest Ct observed (UHV grown at 37°C).

Histological, immunohistochemical (IHC), immunofluorescence (IF) and transmission electron microscopy (TEM) examinations.

For histology and IHC, cultured cells were detached by trypsination and pelleted by centrifugation (2,850 x g, 3 min, RT), then fixed in 2.5% paraformaldehyde (PFA) in 0.2 M phosphate-buffered saline (PBS, pH 7.4) for 24 h at 5°C and routinely paraffin wax embedded. Sections (3-5 µm) were prepared and either stained with hematoxylin-eosin (HE) and examined for the presence of BIBD IB, or used for IHC. Briefly, for IHC, after antigen retrieval with citrate buffer (pH 6.0) in a microwave oven, sections were incubated with affinity-purified rabbit anti-UHV NP (0.25 µg/ml in PBS), followed by HRP-labeled goat anti-rabbit antibody (UltraVision anti-rabbit HRP detection system, Thermo Scientific), with subsequent visualization with diaminobenzidintetrahydrochloride (DAB) and hematoxylin counterstaining as described (10).

Histological and IHC examinations were performed on pellets from two culture flasks for each test in a semi-quantitative fashion. In each complete pellet section (400 x magnification), the proportion of cells with one or more intracytoplasmic IB was graded in 10% steps. The IB size was assessed in µm diameter. Viral NP protein expression was seen in association with IB and, as a more diffuse, but distinct cytoplasmic reaction. Based on the staining intensity within positive cells and the proportion of positive cells, the IHC reaction was graded on a scale from 0.5 to 3, corresponding to a faint (0.5), weak (1), weak to moderate (1.5), moderate (2), moderate to strong (2.5) or strong (3) overall staining intensity. Subsequently, IHC reaction and histology score were combined as indicator of the presence and extent of arenavirus infection in the culture. Scoring was undertaken three times by the same investigator (UH) in a blind fashion.

For TEM, cells were scraped from the flasks and pellets prepared as above, fixed in 1.5% glutaraldehyde buffered in 0.2 M cacodylic acid buffer, pH 7.3, for 12 h at 5°C, and routinely embedded in epoxy resin. Semi-thin and thin sections were prepared as previously described (10), and the latter were examined for the presence and morphology of BIBD IB, using a Philips CM 100.

For IF, cells were grown and infected either on diagnostic 10-well slides, or in culture vessels, detached by pipetting (tick cells) or by trypsinization (vertebrate cells), washed with PBS, diluted in PBS and dried on slides. After fixation in acetone for 10 min, slides were incubated with the anti-NP and anti-NP-C antibodies diluted in PBS (0.25 µg/ml to 0.5 µg/ml), followed by Alexa Fluor 488-labeled or Alexa Fluor 555-labeled goat anti-rabbit (both 1:1,500 dilution in PBS; Invitrogen) for visualization.

RESULTS

Expression and purification of recombinant UHV NP.

We recently characterized two rabbit antisera raised against UHV purified from cell cultures of boid cells (10). Both antisera reacted also with proteins of boid cells which prompted us to produce and purify protein specific antibodies. For this purpose, we produced UHV NP (rNP, aa 1-582), the N-terminal portion of NP (rNP-N, aa 1-339), and the C-terminal portion of NP (rNP-C aa 346-582) with a histidine-tag, using a baculovirus expression system. Immobilized-metal affinity chromatography (IMAC) under denaturing conditions served to purify the proteins, and SDS-PAGE and immunoblotting with anti-his antibody for estimating the purity of the preparations (Fig. 1, top left and middle panel). While rNP and rNP-C each yielded a single distinct band, rNP-N produced a triplet band of the approximate expected molecular size. It is likely that the triplet band is the result of either secondary modifications (e.g. phosphorylation) or N-terminally fragmented pieces of the desired product (his-tag is located in the C-terminus), since all bands of the triplet were recognized by the anti-his antibody (Fig. 1, top middle panel).

The rNP coupled to CnBr Sepharose was used to affinity purify anti-NP PAb from antiserum produced against UHV (10), and NP specific PAbs from antisera produced against rNP-N and rNP-C. The anti-NP reacted strongly with infected cell lysates and rNP, and rNP-C elicited a much stronger immunoreaction than rNP-N (Fig. 1, top right panel), indicating epitope predominance in the C-terminus of NP. The PAbs purified from rNP-N and rNP-C antisera were further labelled with HRP to facilitate the direct use in downstream assays. Both anti-rNP-N and anti-tNP-C were found to react with NP from infected cells and with rNP (Fig. 1, lower panels). Both anti-rNP-

N weakly reacted with rNP-C and vice versa (Fig. 1, lower panels), most probably due to the presence of his-tag in both proteins.

UHV infects cells at 30˚C but growth is limited or hindered at 37˚C.

In our recent paper we demonstrated that UHV not only grows in boid cells, but can also infect and be adapted to grow in Vero E6 cells (10). Initial attempts at infecting the cells with UHV under standard culturing conditions (5% CO_2, 37˚C) had been unsuccessful, whereas maintenance under conditions similar to those applied to the boid cells (10), i.e. at ambient temperatures between 27˚C and 30˚C, resulted in accumulation of UHV antigens. We thus infected both boid kidney and Vero E6 cells with UHV (both Vero E6- and boa cell-adapted UHV), incubated the cells at either 30˚C or 37˚C, and monitored the virus growth by immunoblotting to detect the accumulation of NP. When grown at 30˚C, both cell lines express NP already 2 days post infection (dpi), whereas no NP is detected in cells grown at 37˚C (Fig. 2), indicating that growth is inhibited or markedly hindered at the higher temperature.

Productive UHV infection is reflected in presence, size and quantity of inclusion bodies and viral NP expression.

A specific feature of BIBD is the formation of variably sized eosinophilic intracytoplasmic IB (10). To further characterize the IB, to establish their requirements for active replication, and to assess whether adaptation to Vero E6 cells impairs the ability of UHV to infect boid cells, we collected boid and Vero E6 cells infected with boa- and Vero E6-adapted UHV (boa-UHV and Vero-UHV, respectively) at 8 dpi and analysed them both light microscopically (histology, IF, IHC) and ultrastructurally (TEM). The most relevant quantitative results are summarised in Table 1.

Regardless of the ambient temperature, boid kidney cells infected with boa-UHV exhibited variably sized (0.5 -3.5 μm) IB in a moderate proportion (up to 40%) of cells, whereas viral NP expression was obvious in more than 50% of the cells, with an overall weak to moderate expression intensity (Fig.3A). When consistently maintained at 30°C Vero-UHV induced a more intense infection in the boid cells (up to 80% NP-positive cells and moderate NP expression intensity; Fig. 3B). In contrast, incubation at 37°C reduced both the proportion of cells with IB and the degree of NP expression. This was most pronounced in cells consistently maintained at 37°C, when IB were often barely visible and only faint NP expression confirmed infection of the cells (Fig. 3C; Table 1). The results show that both boa- and Vero-UHV can productively infect boid cells. However, once the virus is adapted to Vero E6 cells, its replication capacity appears to decline with an increase in ambient temperature.

At a consistent ambient temperature of 30°C, Vero-UHV yielded similar results in Vero E6 cells as boa-UHV in boid kidney cells (up to 40% cells with IB of 0.5 - 3.0 μm diameter, moderate NP expression in up to 40% of cells; Fig. 3D). Boa- UHV infected the Vero E6 cells at 30°C, but with low efficiency, since no more than 20% of cells had developed IB at 8 dpi, and NP was only weakly expressed (Fig. 3E). Incubation at 37°C for any length of time resulted in an even lower efficiency of infection (Table 1). Interestingly, the infection with Vero-UHV seemed to fail when the cells were incubated at 37°C immediately after infection (Table 1). These findings suggest that adaptation of UHV to Vero E6 cells is associated with loss of its capacity to infect and grow in these cells at 37°C, perhaps through selection during adaptation.

The ultrastructural characteristics of the IB were very similar irrespective of the infected cell line or the virus isolate used when cells were grown at 37°C (Fig 4). The kinetics of IB formation appeared to be similar in both cell lines. At 8 dpi, the

majority of IB were of irregular shape. By 12 dpi, they had acquired the round to ovoid shape of the IB typically seen in cells of boids with BIBD (10). At this stage, the number of IB overall appeared to be lower than at 8 dpi (data not shown).

Exposure of infected cells to higher ambient temperatures leads to a decrease in the amount of NP.

Since growth of UHV was found to be impaired at 37˚C, we decided to more closely investigate the effect of a temperature rise to 37˚C on cells infected and initially grown at 30˚C. We therefore passaged UHV-infected cells at 15 dpi (boid cells) and 12 dpi (Vero E6 cells) and incubated the new plates at either 30˚C or 37˚C. UHV replication was monitored at 2-day intervals by quantifying the amount of UHV NP in cells using immunoblotting. The temperature increase to 37˚C was associated with a gradual, time-dependent decrease in the amount of UHV NP in cells, indicating that the higher temperature adversely affected the replication of UHV (Fig. 5A). The observed decrease in NP also indicates that the cells lose the accumulated NP deposits likely through the normal cell turnover, since cytopathic effects were not seen. This would suggest that the IB are indeed dynamic complexes, and essential for replication (13).

To analyse whether the decrease in NP would be due to impaired replication of the virus, we compared the amount of viral RNA (both genomic and anti-genomic) after incubation at different temperatures. We infected boid cells with boa-UHV, incubated them at 30˚C or 37˚C for 5 d, and then transferred a plate of cells grown at 30˚C to 37˚C, and vice versa. Cells maintained at 30˚C and 37˚C for the entire examination period served as controls. Samples collected daily up to 8 dpi were analysed by qPCR using UHV Z protein-specific primers which showed that UHV replication is dramatically reduced at 37˚C (Fig. 5B); however, when such cells were transferred to

30˚C after 5 d, replication restarted. When cells grown at 30˚C were transferred to 37˚C, the amount of viral RNA decreased; interestingly, the amount of viral RNA started to increase again after 4 d at the higher temperature, after the initial decrease but at levels approximately 20-40 times lower than in cells grown at 30˚C. Despite the modest recovery of RNA levels (Fig 5B), no protein expression was seen in cells grown at 37˚C (Fig. 2).

UHV originates from a chronically-infected boid bone marrow cell line passaged for more than 10 years at temperatures between 27˚C and 30˚C (10). Therefore, in order to exclude previous cell culture adaptation to a specific temperature range, we decided to study the temperature preference of a recently isolated, genetically distant, BIBDAV (T10404; from snake no. 5 in (10)). We infected both Vero E6 and boid cells with T10404 and maintained the cultures at 30˚C or 37˚C; at 4 dpi we performed temperature swaps and monitored virus growth in samples collected at 5, 7, and 9 dpi as above. The progressive decline in the amount of NP indicates that also the replication of T10404 is impaired in both cell types at 37˚C (Fig. 5C, lanes 2, 5 and 8) in comparison to cells grown at 30˚C (Fig. 5C, lanes 1, 4 and 7). Different from the Vero E6 cells, boid cells inoculated with the virus at 37˚C started to produce virus once transferred to 30˚C (Fig. 5C, lanes 3, 6 and 9), suggesting that, similar to UHV, T10404 retains its infectivity and/or replicates at a low level in boid cells at a higher temperature.

UHV infects cells from different animal classes.

To further investigate the potential of BIBDAV to infect cells other than boid and non-human primate cells (Vero E6), we infected a range of cell lines originating from different animal classes (mammalian, arthropod) with UHV. We wanted to test replication of BIBDAV in arthropod cells, since BIBD epidemics are often

concomitant with snake mite infestation (25), and snake mites could act as a vector for BIBDAV. Since mite cells are not available, we used tick cell lines instead. We found evidence of UHV growth (NP production) by both IF (Fig. 6A) and immunoblots (Fig. 6B) in both mammalian (Vero, Vero E6, A549 and BHK-21) and arthropod (tick cell lines RAE/CTVM1 from *R. appendiculatus*, IRE/CTVM19 from *I. ricinus*, and BME/CTVM2 from *R.* (*B.*) *microplus*) cells when they were propagated at 30˚C, indicating that these cells are permissive for UHV. Curiously, also human cells were found permissive for UHV previously propagated in boid but not in Vero E6 cells. These results highlight the potential of arenaviruses to cross species barriers.

DISCUSSION

BIBD is a fatal disease of boid snakes that is morphologically characterized by the formation of typical intracytoplasmic IB. Recent studies have provided convincing evidence that arenaviruses are the causative agents of BIBD; however, the reservoir host of BIBDAV - if any host exists besides boid snakes themselves - is still unknown. For classical arenaviruses the known reservoir hosts are mammals, i.e. rodents, and for one arenavirus (Tacaribe virus) a bat (4). The isolation of BIBDAV from and in cells of a different taxonomic class, reptiles, i.e. snakes, suggested that arenaviruses might have considerable ability to cross species barriers (10). With this in mind we tested UHV for its ability to infect a panel of cell lines from mammalian and arthropod species, and herein report that BIBDAV can indeed infect cells of various animal classes. Furthermore, we demonstrate that the replication of BIBDAV is temperature-sensitive regardless of the cell type and virus strain used.

The fact that BIBDAV, which like all other arenaviruses in their hosts, cause systemic infections in the snakes, replicate effectively at 30˚C but less or not at all at 37˚C indicates that the body temperature of the reservoir host of these viruses is lower than 37˚C. Mammals are endothermic with body temperatures close to 37˚C except when hibernating, suggesting that the BIBDAV reservoir hosts might not be mammals. In contrast, snakes are exothermic and can therefore provide a suitable ambient temperature range to promote the effective growth of BIBDAV. Captive boid snakes are commonly housed under controlled temperature conditions (typically 25°C at night and 27-31˚C during the day), which we have shown would support the replication of BIBDAV. This could explain the high susceptibility of captive boids to these viruses. In contrast, wild snakes are exposed to a broader range of temperatures, and in the case of boids and other snakes known to develop BIBD these are often

386 higher. Our findings thus suggest that in wild snakes the replication of BIBDAV
387 could be restricted or influenced by changes in the ambient temperature, and that the
388 susceptibility of a snake species might actually be related to the environment in which
389 it lives. Chronic infection of the reservoir host is seen with “classical” rodent-borne
390 arenaviruses, and is considered almost a hallmark of the family Arenaviridae.
391 Accordingly, BIBDAV could chronically infect boids living in the wild, however, to
392 our knowledge there is so far no report suggesting this.
393 The occurrence of BIBD in snake collections has been associated with concurrent
394 snake mite (*Ophionyssus natricis*) infestation (25). Since cell lines of this arthropod
395 species are not available, we tested embryo-derived cell lines of three tick species, *I.*
396 *ricinus R. appendiculatus* and *R.* (*B.*) *microplus*, for their susceptibility to UHV.
397 Indeed, all three tick cell lines were found to support UHV replication, which
398 provides the first evidence that BIBDAV could indeed be transmitted by an arthropod
399 vector, i.e. be an arbovirus, with arthropods acting as intermediate or even as reservoir
400 hosts for BIBDAV. This hypothesis is supported by the fact that other arthropod-
401 borne viruses, i.e. members of the *Togaviridae* and *Flaviviridae*, have been found in
402 snakes (26), and arthropods such as ticks and mosquitoes can harbour persistent
403 arbovirus infections in the absence of obvious deleterious effects (27-29). On the
404 other hand, LCMV, another arenavirus, has been shown to productively infect
405 primary tick cell cultures (30), which indicates that tick cells are in general permissive
406 for arenaviruses. Transmission via an arthropod vector would allow BIBDAV, at least
407 in theory, to cross from one host species to another in the wild. It remains to be
408 studied whether snake mites or other blood-sucking parasites, such as ticks, can
409 indeed transmit the virus.

The fact that UHV was able to infect such a broad range of cell lines, and that UHV was still able to infect boid cells after it was adapted to Vero E6 cells through cultivation, is particularly interesting with regards to its potential receptor usage. Curiously, Vero-UHV infected A549 cells with lower efficacy than boa-UHV. Vero E6 cells are known to secrete interferon-lambda (IFN-λ) in response to infection by New World hantaviruses (31). Thus the observed growth restriction of Vero-UHV in A549 cells might be due to inhibitory effects of IFN-λ. As few tools are available for detecting boid proteins or genes, the infection of Vero E6 and A549 cells will facilitate studies on, for example, the interaction of BIBDAV with receptors and innate immunity. Rodent-borne arenaviruses use transferrin receptor 1 (TfR1) and α-dystroglycan as their receptors when infecting man (32, 33). A549 cells are known to express TfR1 and therefore it is of interest to determine whether BIBDAV would use this receptor for their entry. Thus far, nothing is known about the cellular receptor(s) of BIBDAV. However, the ability of UHV to infect various cell lines, and the fact that in snakes with BIBD develop IB in basically all cell types, suggests that the receptor is more or less ubiquitous and conserved throughout animal classes. This would, again in theory, enable the spread of BIBDAV to different classes of animals. Nevertheless, it appears that the spread of these viruses is limited by their growth temperature requirements.

ACKNOWLEDGEMENTS

The authors are grateful to Kirsi Aaltonen, Irina Suomalainen and the technicians in the Finnish Centre for Laboratory Animal Pathology, Faculty of Veterinary Medicine, University of Helsinki, as well as Lisbeth Nufer, TEM Unit, Institute of Veterinary Pathology, Vetsuisse Faculty, University of Zurich, for excellent technical assistance. The authors thank the Tick Cell Biobank, the Pirbright Institute and Dr. Anu Hakala for provision, transfer and cultivation of tick cell lines. The study was supported by the Academy of Finland and the Finnish Foundation for Veterinary Research (2011 and 2012 grant rounds).

REFERENCES

1. **Irwin, N. R., M. Bayerlova, O. Missa, and N. Martinkova.** 2012. Complex patterns of host switching in New World arenaviruses. Mol. Ecol. **21:**4137-4150. doi: 10.1111/j.1365-294X.2012.05663.x; 10.1111/j.1365-294X.2012.05663.x.

2. **Martinez, M. G., M. A. Bialecki, S. Belouzard, S. M. Cordo, N. A. Candurra, and G. R. Whittaker.** 2013. Utilization of human DC-SIGN and L-SIGN for entry and infection of host cells by the New World arenavirus, Junin virus. Biochem. Biophys. Res. Commun. **441:**612-617. doi: 10.1016/j.bbrc.2013.10.106; 10.1016/j.bbrc.2013.10.106.

3. **Rieger, T., D. Merkler, and S. Gunther.** 2013. Infection of type I interferon receptor-deficient mice with various old world arenaviruses: a model for studying virulence and host species barriers. PLoS One. **8:**e72290. doi: 10.1371/journal.pone.0072290; 10.1371/journal.pone.0072290.

4. **Moraz, M. L., and S. Kunz.** 2011. Pathogenesis of arenavirus hemorrhagic fevers. Expert Rev. Anti Infect. Ther. **9:**49-59. doi: 10.1586/eri.10.142.

5. **Briese, T., J. T. Paweska, L. K. McMullan, S. K. Hutchison, C. Street, G. Palacios, M. L. Khristova, J. Weyer, R. Swanepoel, M. Egholm, S. T. Nichol, and W. I. Lipkin.** 2009. Genetic detection and characterization of Lujo virus, a new hemorrhagic fever-associated arenavirus from southern Africa. PLoS Pathog. **5:**e1000455. doi: 10.1371/journal.ppat.1000455.

6. **Nunberg, J. H., and J. York.** 2012. The curious case of arenavirus entry, and its inhibition. Viruses. **4:**83-101. doi: 10.3390/v4010083.

7. **Bausch, D. G., C. M. Hadi, S. H. Khan, and J. J. Lertora.** 2010. Review of the literature and proposed guidelines for the use of oral ribavirin as postexposure prophylaxis for Lassa fever. Clin. Infect. Dis. **51:**1435-1441. doi: 10.1086/657315; 10.1086/657315.

8. **Stenglein, M. D., C. Sanders, A. L. Kistler, J. G. Ruby, J. Y. Franco, D. R. Reavill, F. Dunker, and J. L. Derisi.** 2012. Identification, characterization, and in vitro culture of highly divergent arenaviruses from boa constrictors and annulated tree boas: candidate etiological agents for snake inclusion body disease. MBio. **3:**e00180-12. doi: 10.1128/mBio.00180-12; 10.1128/mBio.00180-12.

9. **Bodewes, R., M. J. Kik, V. S. Raj, C. M. Schapendonk, B. L. Haagmans, S. L. Smits, and A. D. Osterhaus.** 2013. Detection of novel divergent arenaviruses in boid snakes with inclusion body disease in The Netherlands. J. Gen. Virol. **94:**1206-1210. doi: 10.1099/vir.0.051995-0; 10.1099/vir.0.051995-0.

10. **Hetzel, U., T. Sironen, P. Laurinmaki, L. Liljeroos, A. Patjas, H. Henttonen, A. Vaheri, A. Artelt, A. Kipar, S. J. Butcher, O. Vapalahti, and J. Hepojoki.** 2013. Isolation, identification, and characterization of novel arenaviruses, the etiological agents of boid inclusion body disease. J. Virol. **87:**10918-10935. doi: 10.1128/JVI.01123-13; 10.1128/JVI.01123-13.

11. **Wozniak, E., J. McBride, D. DeNardo, R. Tarara, V. Wong, and B. Osburn.** 2000. Isolation and Characterization of an Antigenically Distinct 68- kd Protein from Nonviral Intracytoplasmic Inclusions in Boa Constrictors Chronically Infected with

483 the Inclusion Body Disease Virus (IBDV: Retroviridae). Veterinary Pathology
484 Online. **37:**449-459. doi: 10.1354/vp.37-5-449.

485 12. **Schumacher, J., E. R. Jacobson, B. L. Homer, and J. M. Gaskin.** 1994.
486 Inclusion Body Disease in Boid Snakes. Journal of Zoo and Wildlife Medicine. **25:**pp.
487 511-524.

488 13. **Baird, N. L., J. York, and J. H. Nunberg.** 2012. Arenavirus infection induces
489 discrete cytosolic structures for RNA replication. J. Virol. **86:**11301-11310. doi:
490 10.1128/JVI.01635-12.

491 14. **Charrel, R. N., B. Coutard, C. Baronti, B. Canard, A. Nougairede, A.**
492 **Frangeul, B. Morin, S. Jamal, C. L. Schmidt, R. Hilgenfeld, B. Klempa, and X.**
493 **de Lamballerie.** 2011. Arenaviruses and hantaviruses: from epidemiology and
494 genomics to antivirals. Antiviral Res. **90:**102-114. doi:
495 10.1016/j.antiviral.2011.02.009.

496 15. **Urata, S., and J. Yasuda.** 2012. Molecular mechanism of arenavirus assembly
497 and budding. Viruses. **4:**2049-2079. doi: 10.3390/v4102049; 10.3390/v4102049.

498 16. **Bodewes, R., V. S. Raj, M. J. Kik, C. M. Schapendonk, B. L. Haagmans, S. L.**
499 **Smits, and A. D. Osterhaus.** 2014. Updated phylogenetic analysis of arenaviruses
500 detected in boid snakes. J. Virol. **88:**1399-1400. doi: 10.1128/JVI.02753-13;
501 10.1128/JVI.02753-13.

502 17. **Hetzel, U., T. Sironen, P. Laurinmaki, L. Liljeroos, A. Patjas, H. Henttonen,**
503 **A. Vaheri, A. Artelt, A. Kipar, S. J. Butcher, O. Vapalahti, and J. Hepojoki.**
504 2014. Reply to "updated phylogenetic analysis of arenaviruses detected in boid
505 snakes". J. Virol. **88:**1401-13. doi: 10.1128/JVI.03044-13; 10.1128/JVI.03044-13.

506 18. **Burri, D. J., J. R. Palma, S. Kunz, and A. Pasquato.** 2012. Envelope
507 glycoprotein of arenaviruses. Viruses. **4:**2162-2181. doi: 10.3390/v4102162;
508 10.3390/v4102162.

509 19. **Huiskonen, J. T., J. Hepojoki, P. Laurinmaki, A. Vaheri, H. Lankinen, S. J.**
510 **Butcher, and K. Grunewald.** 2010. Electron cryotomography of Tula hantavirus
511 suggests a unique assembly paradigm for enveloped viruses. J. Virol. **84:**4889-4897.
512 doi: 10.1128/JVI.00057-10.

513 20. **Bell-Sakyi, L., E. Zweygarth, E. F. Blouin, E. A. Gould, and F. Jongejan.**
514 2007. Tick cell lines: tools for tick and tick-borne disease research Trends Parasitol.
515 **23:**450-457. doi: S1471-4922(07)00191-2 [pii].

516 21. **Pedra, J. H., S. Narasimhan, D. Rendic, K. DePonte, L. Bell-Sakyi, I. B.**
517 **Wilson, and E. Fikrig.** 2010. Fucosylation enhances colonization of ticks by
518 Anaplasma phagocytophilum Cell. Microbiol. **12:**1222-1234. doi: 10.1111/j.1462-
519 5822.2010.01464.x [doi].

520 22. **Bell-Sakyi, L.** 2004. Ehrlichia ruminantium grows in cell lines from four ixodid
521 tick genera J. Comp. Pathol. **130:**285-293. doi: 10.1016/j.jcpa.2003.12.002 [doi].

522 23. **Levingston Macleod, J. M., A. D'Antuono, M. E. Loureiro, J. C. Casabona,**
523 **G. A. Gomez, and N. Lopez.** 2011. Identification of two functional domains within
524 the arenavirus nucleoprotein. J. Virol. **85:**2012-2023. doi: 10.1128/JVI.01875-10;
525 10.1128/JVI.01875-10.

24. **Hastie, K. M., T. Liu, S. Li, L. B. King, N. Ngo, M. A. Zandonatti, V. L. Woods Jr, J. C. de la Torre, and E. O. Saphire.** 2011. Crystal structure of the Lassa virus nucleoprotein-RNA complex reveals a gating mechanism for RNA binding. Proc. Natl. Acad. Sci. U. S. A. **108:**19365-19370. doi: 10.1073/pnas.1108515108; 10.1073/pnas.1108515108.

25. **Chang, L., and E. R. Jacobson.** 2010. Inclusion Body Disease, A Worldwide Infectious Disease of Boid Snakes: A Review. Journal of Exotic Pet Medicine. **19:**216-225. doi: 10.1053/j.jepm.2010.07.014.

26. **Essbauer, S., and W. Ahne.** 2001. Viruses of lower vertebrates J. Vet. Med. B Infect. Dis. Vet. Public Health. **48:**403-475.

27. **Labuda, M., and P. A. Nuttall.** 2004. Tick-borne viruses Parasitology. **129 Suppl:**S221-45.

28. **Blair, C. D.** 2011. Mosquito RNAi is the major innate immune pathway controlling arbovirus infection and transmission Future Microbiol. **6:**265-277. doi: 10.2217/fmb.11.11 [doi].

29. **Ballinger, M. J., J. A. Bruenn, J. Hay, D. Czechowski, and D. J. Taylor.** 2014. Discovery and evolution of bunyavirids in arctic phantom midges and ancient bunyavirid-like sequences in insect genomes. J. Virol. **88:**8783-8794. doi: 10.1128/JVI.00531-14 [doi].

30. **Rehacek, J.** 1965. Cultivation of different viruses in tick tissue cultures. Acta Virol. **9:**332-337.

31. **Prescott, J., P. Hall, M. Acuna-Retamar, C. Ye, M. G. Wathelet, H. Ebihara, H. Feldmann, and B. Hjelle.** 2010. New World hantaviruses activate IFNlambda production in type I IFN-deficient vero E6 cells. PLoS One. **5:**e11159. doi: 10.1371/journal.pone.0011159.

32. **Radoshitzky, S. R., J. Abraham, C. F. Spiropoulou, J. H. Kuhn, D. Nguyen, W. Li, J. Nagel, P. J. Schmidt, J. H. Nunberg, N. C. Andrews, M. Farzan, and H. Choe.** 2007. Transferrin receptor 1 is a cellular receptor for New World haemorrhagic fever arenaviruses. Nature. **446:**92-96. doi: 10.1038/nature05539.

33. **Choe, H., S. Jemielity, J. Abraham, S. R. Radoshitzky, and M. Farzan.** 2011. Transferrin receptor 1 in the zoonosis and pathogenesis of New World hemorrhagic fever arenaviruses. Curr. Opin. Microbiol. **14:**476-482. doi: 10.1016/j.mib.2011.07.014; 10.1016/j.mib.2011.07.014.

559 **FIGURE LEGENDS**

560 **Figure 1.** UHV recombinant proteins. The top left panel shows recombinant NP
561 (rNP), rNP-N (N-terminal fragment of NP, aa 1-339) and rNP-C (C-terminal fragment
562 of NP, aa 346-582) IMAC-purified under denaturing conditions as separated by SDS-
563 PAGE and visualized by Coomassie Brilliant Blue staining. The top middle and right
564 panels show immunoblots with anti-His tag and affinity purified anti-UHV NP
565 antibodies respectively. Bottom left and right panels show immunoblots with affinity
566 purified anti-rNP-N and anti-rNP-C antibodies, respectively. The immunoblots were
567 visualized by Odyssey Infrared Imaging System (LI-COR).

568 **Figure 2.** Temperature restricts BIBDAV growth in boid and Vero E6 cells. Boid and
569 Vero E6 cells were infected with Vero-UHV and cultured at 30 ˚C or 37 ˚C. Cells
570 were collected in lysis buffer and 10 μg of total protein from each time point was
571 analysed by immunoblotting using HRP-labelled anti-rNP-C antibody. The results
572 were recorded on X-ray film utilizing ECL.

573 **Figure 3.** Morphological features and BIBDAV NP expression in UHV-infected cell
574 cultures at 8 dpi. **A-C)** Permanent cell line I/1Ki derived from boid kidney cells. **A)**
575 Infection with boa-UHV and incubation at 30°C. Viral NP expression is observed in
576 more than 50% of the cells, with an overall weak to moderate staining intensity. NP
577 expression is also seen in the inclusion bodies (arrows); inset: variably sized inclusion
578 bodies as evident in HE stained sections (arrowheads). **B**) Infection with Vero-UHV
579 and incubation at 30°C. Around 80% of cells exhibit NP expression, and with overall
580 moderate staining intensity. **C)** Cells maintained at 37°C for 8 d. NP expression is
581 mainly seen as a faint diffuse cytoplasmic staining in a few cells (arrows) or, rarely,
582 as very small cytoplasmic inclusion bodies (arrowhead; score 0.5; **D, E**). African
583 Green Monkey (Vero E6) cells after UHV infection and culture at 30°C for 8 d. **D)**

584 Infection with Vero-UHV. Viral NP expression is observed in approximately 40% of
585 the cells, with an overall moderate staining intensity. NP Inset: variably sized
586 inclusion bodies as evident in HE stained sections (arrowheads). **E)** Infection with
587 boa-UHV results in the formation of small IB that are only visible when stained for
588 NP expression (arrows); NP expression is seen in less than 20% of cells, and with
589 generally weak intensity. HRP method, hematoxylin counterstain, Bars = 20 μm;
590 insets: HE stain.

591 **Figure 4.** Ultrastructural features of boid kidney cells cells (**A**: mock infected; **B**: boa-
592 UHV infected) and Vero E6 cells (**C**: mock infected; **D**; Vero-UHV infected). Cells
593 were maintained at 30°C for 8 dpi. In boid kidney cells (**B**), IB appear as several
594 irregularly shaped intracytoplasmic structures (arrows). In the Vero E6 cells (**D**), they
595 are round to ellipsoid (arrows). Bars = 2 μm.

596 **Figure 5.** The effect of ambient temperature on the growth of UHV and T10404. **A)**
597 Boid and Vero E6 cells infected with UHV (15 dpi and 12 dpi, respectively) were
598 transferred to fresh 6-well plates and grown at 30˚C or 37˚C. Cells were collected at
599 two day interval in lysis buffer and 10 μg of total protein from each time point was
600 analysed by immunoblotting using HRP-labelled anti-rNP-C antibody. The results
601 were recorded on X-ray film utilizing ECL. **B)** Boid cells were infected with UHV
602 and grown at 30˚C or 37˚C. At 5 dpi a plate of cells grown at 37˚C was transferred to
603 30˚C and a plate of cells grown at 30˚C to 37˚C. Infected cells constantly kept at 30˚C
604 or 37˚C were used as controls. RNA isolated from cells collected at 5, 6, 7, and 8 dpi
605 (x-axis) was quantified with qPCR using UHV Z protein-specific primers. The results
606 are shown as fold increase in comparison to the vRNA level of cells grown at 37˚C (2
607 dpi, the highest Ct value measured). **C)** Boid and Vero E6 cells were infected with
608 T10404 and cultured at 30˚C or 37˚C. At 4 dpi the cells grown at 37˚C were

609 transferred to 30˚C (37˚C=>30˚C), and a plate of cells grown at 30˚C was transferred
610 to 37˚C (30 ˚C=>37˚C). Infected cells kept constantly at 30˚C were used as positive
611 controls. Cells were collected in lysis buffer and 10 µg of total protein from each time
612 point was analysed by immunoblotting using affinity purified anti-UHV NP antibody
613 (anti-rNP-N and anti-rNP-C yielded lower signal intensity). The immunoblot was
614 recorded using Odyssey Infrared Imaging System (LI-COR).
615 **Figure 6.** Susceptibility of different cell lines to UHV infection. BME/CTVM2 (*R.*
616 [*B.*] *microplus* embryo), RAE/CTVM1 (*R. appendiculatus* embryo), IRE/CTVM19 (*I.*
617 *ricinus* embryo) BHK-21 (baby hamster kidney), Vero (African green monkey
618 kidney), and A549 (human lung adenocarcinoma) cells were infected with UHV and
619 grown at 30˚C. A) Infected (UHV) and non-infected (mock) cells were fixed (at 8 dpi
620 for BHK and Vero, 14 dpi for tick cell lines, and 3 dpi for A549) and stained with
621 anti-rNP-C polyclonal antibody in conjugation with anti-rabbit AlexaFluor 488-
622 labeled secondary antibody. The cells were imaged at 400x magnification. B)
623 Immunoblot of UHV-infected tick and BHK21-cells on left panel and A549 cells on
624 right panel. The cells were collected (at 8 dpi for BHK, 14 dpi for tick cell lines, and
625 at 1 and 3 dpi for A549) in lysis buffer and 10 µg of total protein analysed by
626 immunoblotting with affinity purified anti-UHV NP antibody as recorded by Odyssey
627 Infrared Imaging System (LI-COR).
628

Table 1. Results of the semi-quantitative assessment of BIBDAV infection of boid kidney and Vero E6 cells with boa- and Vero-UHV maintained at different ambient temperatures for 8 days, based on the proportion of cells with IB and the extent of *in situ* NP expression.

Cell type	Virus used	30°C (8d)		30°C (4d) → 37°C (4d)		37°C (8d)		37°C (4d) → 30°C (4d)	
		N (%)	IHC	N (%)	IHC	N (%)	IHC	N (%)	IHC
Boid kidney	Boa-UHV	> 30 - 40	1.5	> 30 - 40	1.5	> 30 - 40	1.0	> 20 - 30	1.0
	Vero-UHV	> 40 - 50	2.0	> 10 - 20	1.5	≤ 10	0.5	> 20 - 30	1.0
Vero E6	Boa-UHV	> 10 - 20	1.0	≤ 10	0.5	≤ 10	0.5	≤ 10	0.5
	Vero-UHV	> 30 - 40	2.0	≤ 10	1.0	-	-	-	-

Scoring based on: **N** - percentage of cells with IB. **IHC** - *in situ*, i.e. immunohistochemical expression of BIBDAV NP antigen, graded as faint (0.5), weak (1), weak to moderate (1.5), moderate (2), moderate to strong (2.5) and strong (3) based on the staining intensity within positive cells and the proportion of positive cells.

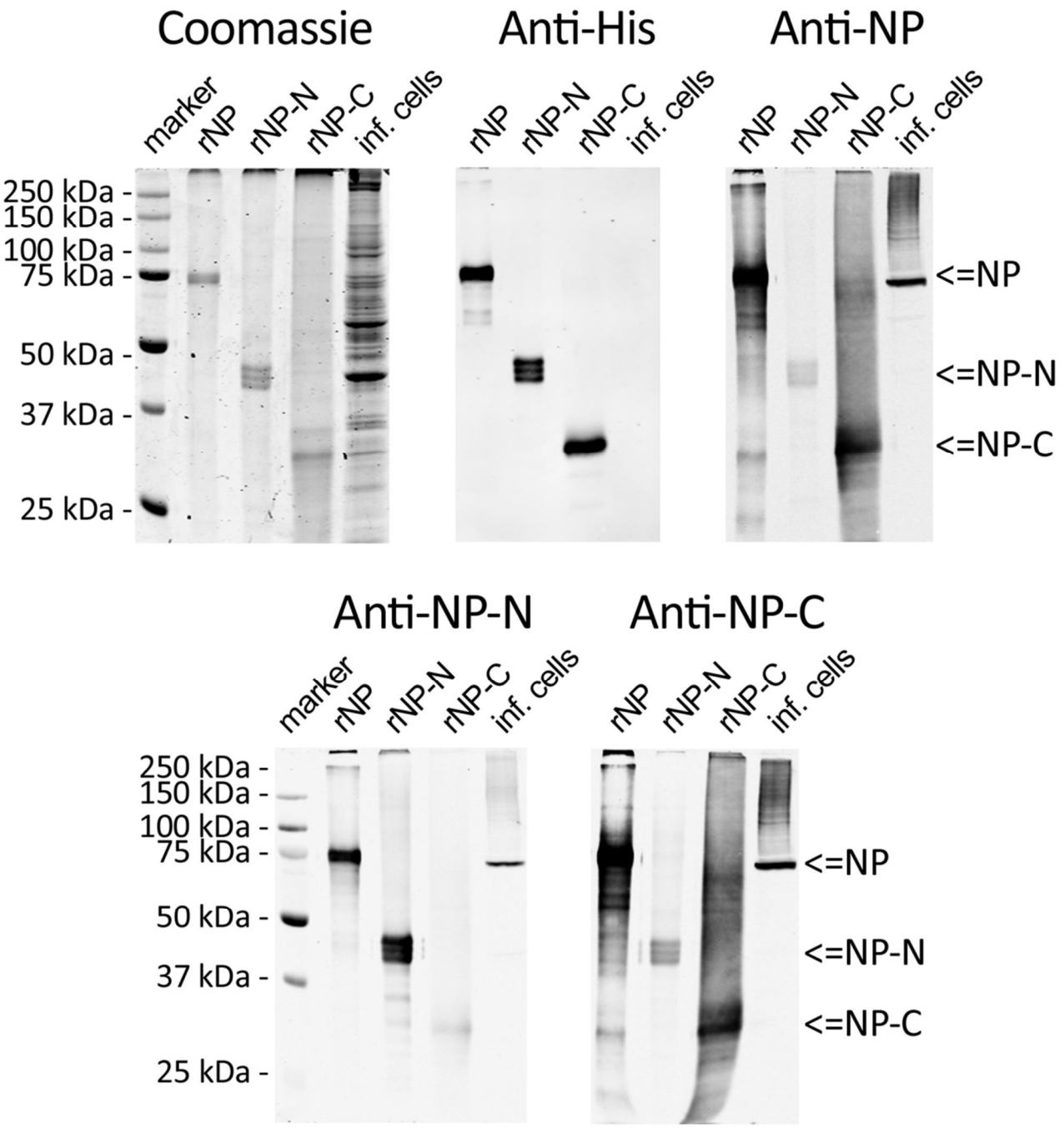

Figure 1. UHV recombinant proteins. The top left panel shows recombinant NP (rNP), rNP-N (N-terminal fragment of NP, aa 1-339) and rNP-C (C-terminal fragment of NP, aa 346-582) IMAC-purified under denaturing conditions as separated by SDS-PAGE and visualized by Coomassie Brilliant Blue staining. The top middle and right panels show immunoblots with anti-His tag and affinity purified anti-UHV NP antibodies respectively. Bottom left and right panels show immunoblots with affinity purified anti-rNP-N and anti-rNP-C antibodies, respectively. The immunoblots were visualized by Odyssey Infrared Imaging System (LI-COR).

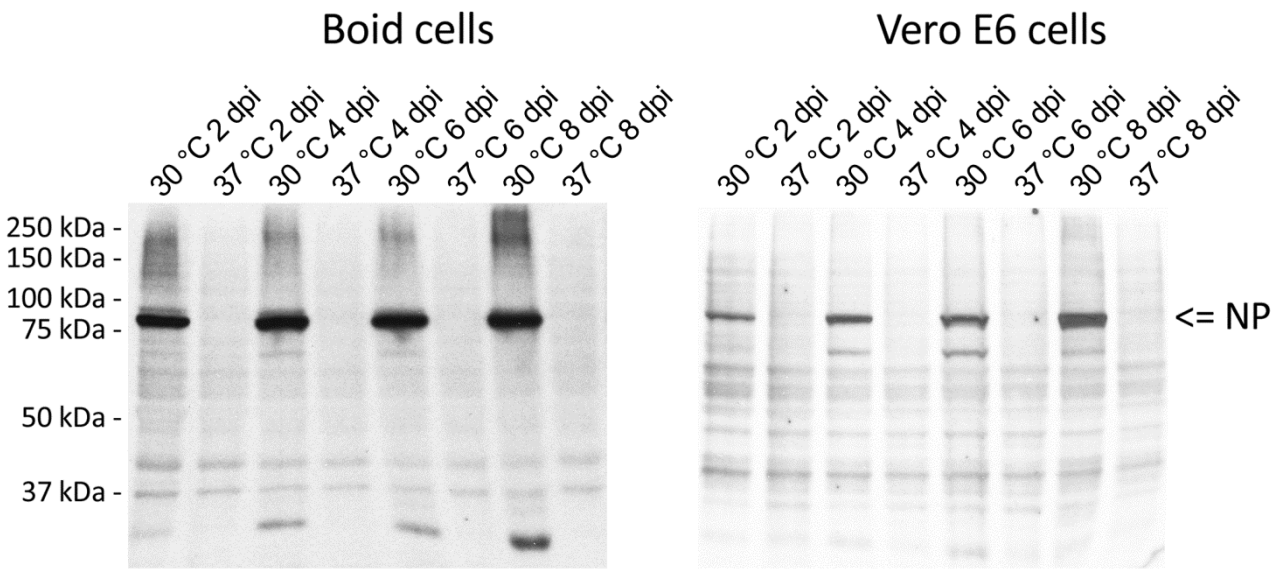

Figure 2. Temperature restricts BIBDAV growth in boid and Vero E6 cells. Boid and Vero E6 cells were infected with Vero-UHV and cultured at 30 ˚C or 37 ˚C. Cells were collected in lysis buffer and 10 µg of total protein from each time point was analysed by immunoblotting using HRP-labelled anti-rNP-C antibody. The results were recorded on X-ray film utilizing ECL.

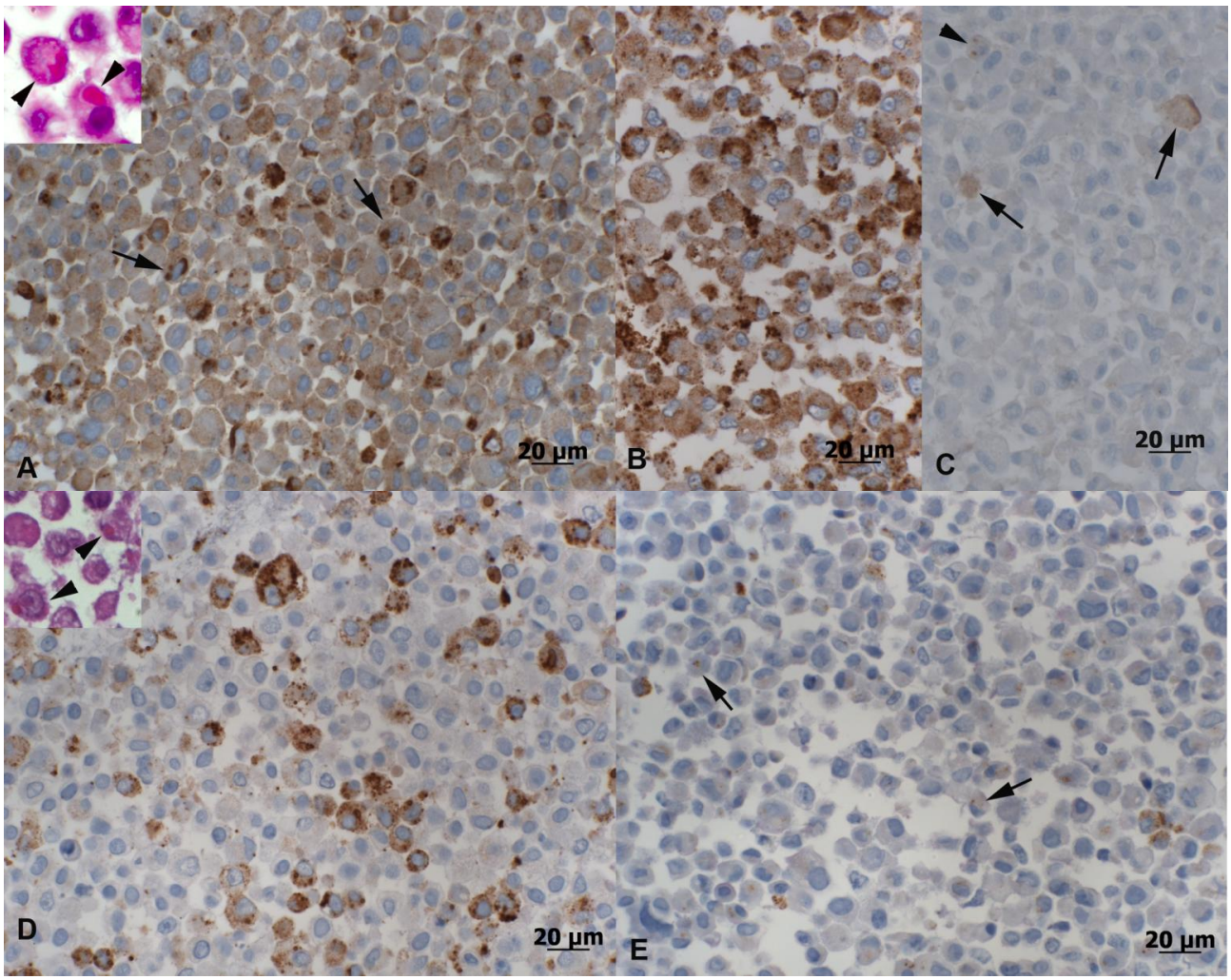

Figure 3. Morphological features and BIBDAV NP expression in UHV-infected cell cultures at 8 dpi. **A-C)** Permanent cell line I/1Ki derived from boid kidney cells. **A)** Infection with boa-UHV and incubation at 30°C. Viral NP expression is observed in more than 50% of the cells, with an overall weak to moderate staining intensity. NP expression is also seen in the inclusion bodies (arrows); inset: variably sized inclusion bodies as evident in HE stained sections (arrowheads). **B**) Infection with Vero-UHV and incubation at 30°C. Around 80% of cells exhibit NP expression, and with overall moderate staining intensity. **C)** Cells maintained at 37°C for 8 d. NP expression is mainly seen as a faint diffuse cytoplasmic staining in a few cells (arrows) or, rarely, as very small cytoplasmic inclusion bodies (arrowhead; score 0.5; **D, E**). African Green Monkey (Vero E6) cells after UHV infection and culture at 30°C for 8 d. **D)** Infection with Vero-UHV. Viral NP expression is observed in approximately 40% of the cells, with an overall moderate staining intensity. NP Inset: variably sized inclusion bodies as evident in HE stained sections (arrowheads). **E)** Infection with boa-UHV results in the formation of small IB that are only visible when stained for NP expression (arrows); NP expression is seen in less than 20% of cells, and with generally weak intensity. HRP method, hematoxylin counterstain, Bars = 20 µm; insets: HE stain.

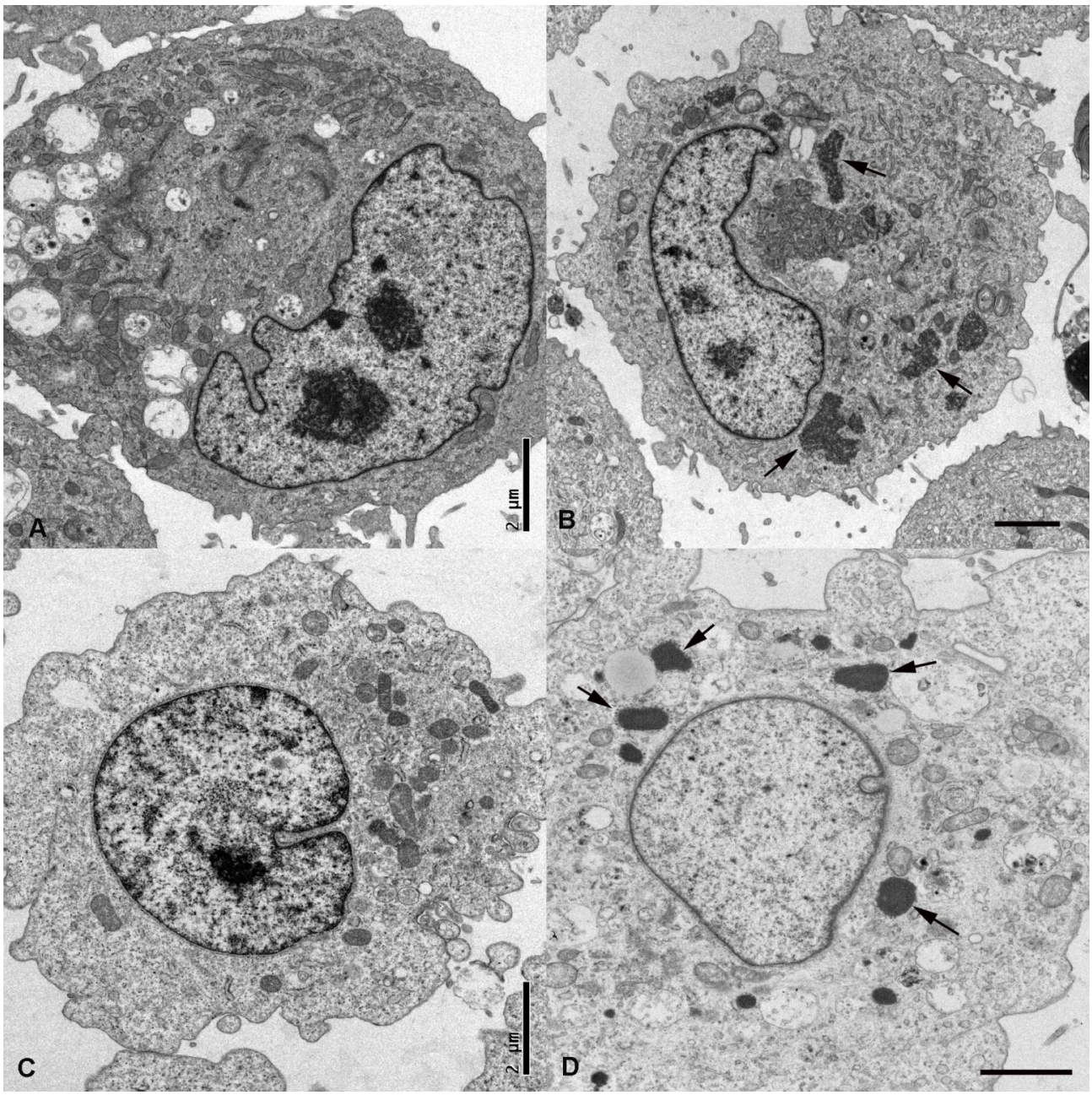

Figure 4. Ultrastructural features of boid kidney cells cells (**A**: mock infected; **B**: boa-UHV infected) and Vero E6 cells (**C**: mock infected; **D**; Vero-UHV infected). Cells were maintained at 30°C for 8 dpi. In boid kidney cells (**B**), IB appear as several irregularly shaped intracytoplasmic structures (arrows). In the Vero E6 cells (**D**), they are round to ellipsoid (arrows). Bars = 2 µm.

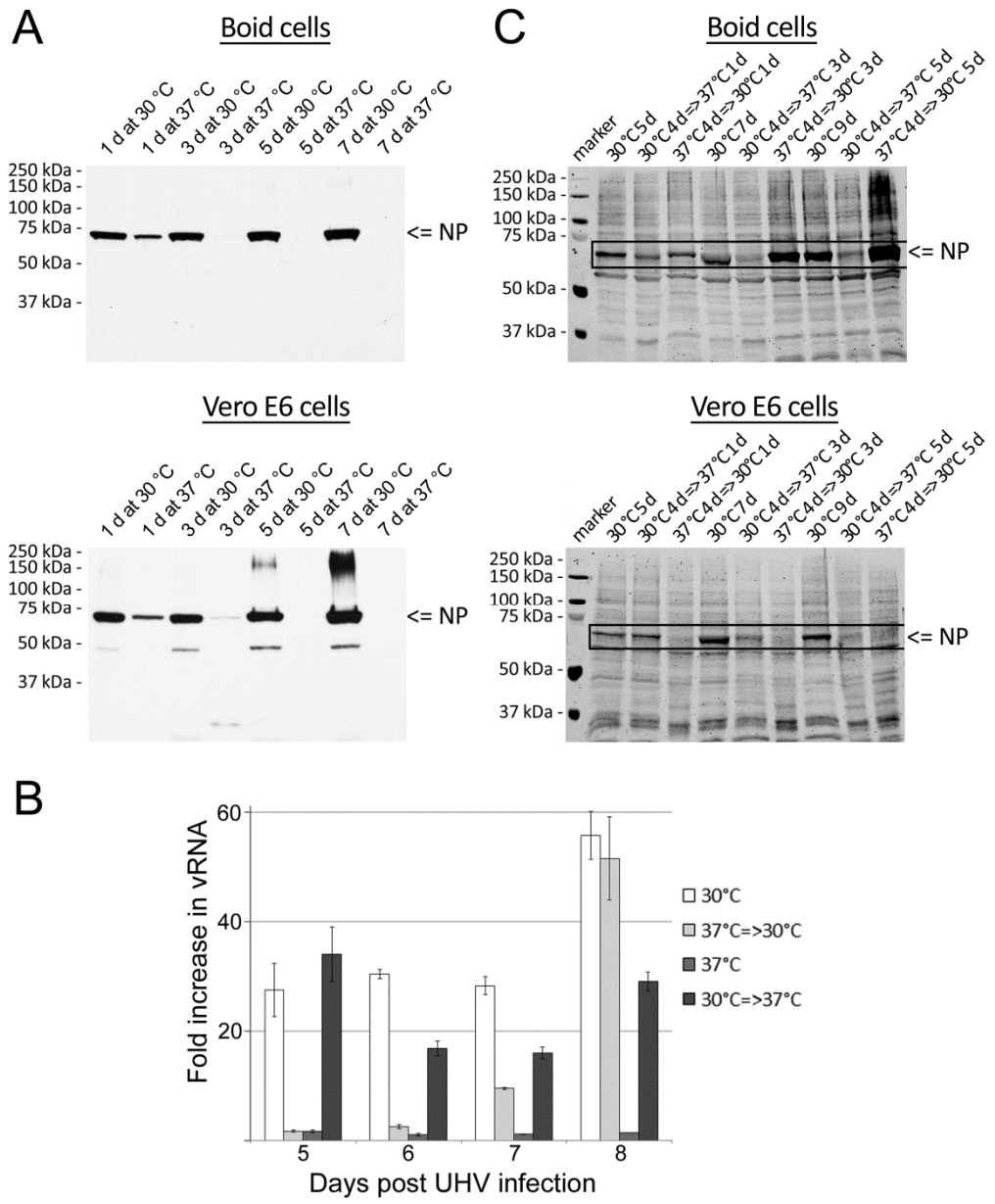

Figure 5. The effect of ambient temperature on the growth of UHV and T10404. **A)** Boid and Vero E6 cells infected with UHV (15 dpi and 12 dpi, respectively) were transferred to fresh 6-well plates and grown at 30˚C or 37˚C. Cells were collected at two day interval in lysis buffer and 10 µg of total protein from each time point was analysed by immunoblotting using HRP-labelled anti-rNP-C antibody. The results were recorded on X-ray film utilizing ECL. **B)** Boid cells were infected with UHV and grown at 30˚C or 37˚C. At 5 dpi a plate of cells grown at 37˚C was transferred to 30˚C and a plate of cells grown at 30˚C to 37˚C. Infected cells constantly kept at 30˚C or 37˚C were used as controls. RNA isolated from cells collected at 5, 6, 7, and 8 dpi (x-axis) was quantified with qPCR using UHV Z protein-specific primers. The results are shown as fold increase in comparison to the vRNA level of cells grown at 37˚C (2 dpi, the highest Ct value measured). **C)** Boid and Vero E6 cells were infected with T10404 and cultured at 30˚C or 37˚C. At 4 dpi the cells grown at 37˚C were transferred to 30˚C (37˚C=>30˚C), and a plate of cells grown at 30˚C was transferred to 37˚C (30 ˚C=>37˚C). Infected cells kept constantly at 30˚C were used as positive controls. Cells were collected in lysis buffer and 10 µg of total protein from each time point was analysed by immunoblotting using affinity purified anti-UHV NP antibody (anti-rNP-N and anti-rNP-C yielded lower signal intensity). The immunoblot was recorded using Odyssey Infrared Imaging System (LI-COR).

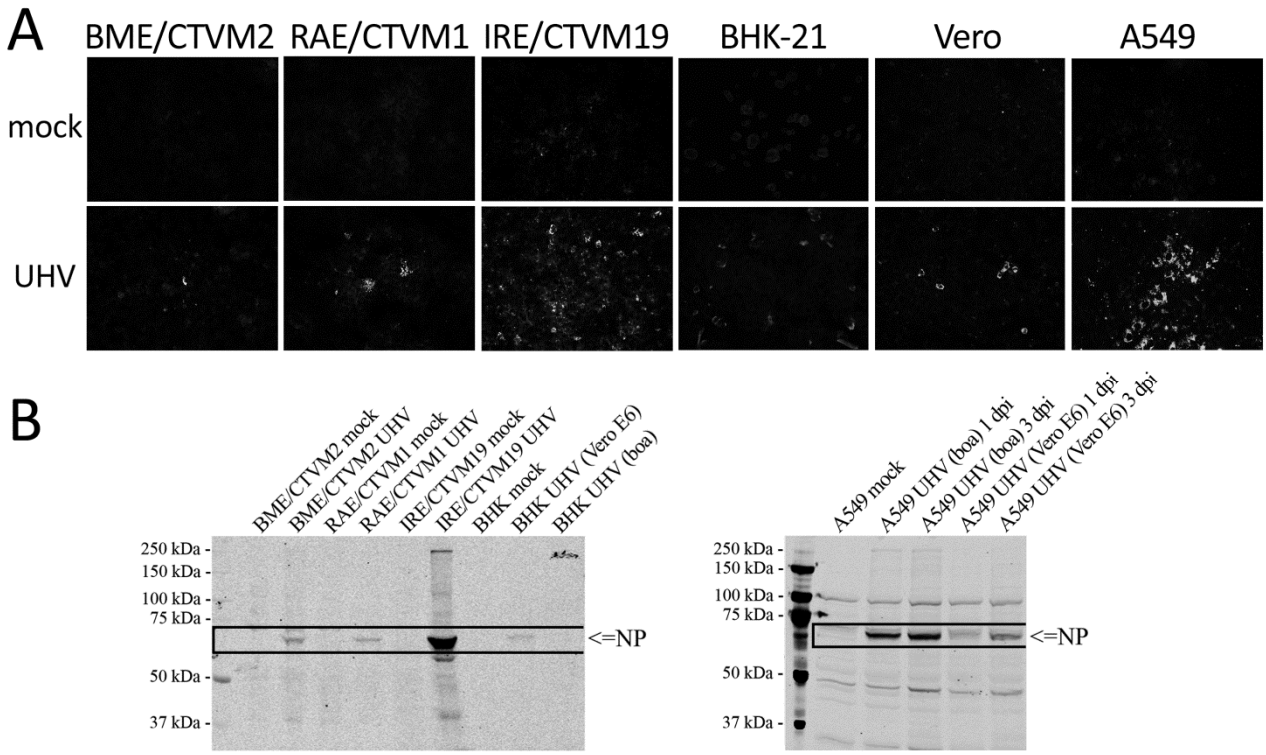

Figure 6. Susceptibility of different cell lines to UHV infection. BME/CTVM2 (*R.* [*B.*] *microplus* embryo), RAE/CTVM1 (*R. appendiculatus* embryo), IRE/CTVM19 (*I. ricinus* embryo) BHK-21 (baby hamster kidney), Vero (African green monkey kidney), and A549 (human lung adenocarcinoma) cells were infected with UHV and grown at 30˚C. A) Infected (UHV) and non-infected (mock) cells were fixed (at 8 dpi for BHK and Vero, 14 dpi for tick cell lines, and 3 dpi for A549) and stained with anti-rNP-C polyclonal antibody in conjugation with anti-rabbit AlexaFluor 488-labeled secondary antibody. The cells were imaged at 400x magnification. B) Immunoblot of UHV-infected tick and BHK21-cells on left panel and A549 cells on right panel. The cells were collected (at 8 dpi for BHK, 14 dpi for tick cell lines, and at 1 and 3 dpi for A549) in lysis buffer and 10 µg of total protein analysed by immunoblotting with affinity purified anti-UHV NP antibody as recorded by Odyssey Infrared Imaging System (LI-COR).